

Soliton dynamics and self-induced transparency in nonlinear nanosuspensions

R. El-Ganainy¹, D. N. Christodoulides¹, C. Rotschild², and M. Segev²

¹College of Optics & Photonics-CREOL, University of Central Florida, Orlando, Florida, 32816

²Physics Department, Technion-Israel Institute of Technology, Haifa 32000, Israel

Corresponding author: demetri@creol.ucf.edu

Abstract: We study spatial soliton dynamics in nano-particle suspensions. Starting from the Nernst-Planck and Smoluchowski equations, we demonstrate that in these systems the underlying nonlinearities as well as the nonlinear Rayleigh losses depend exponentially on optical intensity. Two different nonlinear regimes are identified depending on the refractive index contrast of the nanoparticles involved and the interesting prospect of self-induced transparency is demonstrated. Soliton stability is systematically analyzed for both 1D and 2D configurations and their propagation dynamics in the presence of Rayleigh losses is examined. The possibility of synthesizing artificial nonlinearities using mixtures of nanosuspensions is also considered.

©2007 Optical Society of America

OCIS codes: (190.3970) Microparticle nonlinear optics, (190.5940) Self action effects, (290.5870) Scattering, Rayleigh.

References and links

1. G. G. Hammes, *Thermodynamics and Kinetics for the Biological Sciences*, (John Wiley and Sons 2000).
2. P.W. Smith, A. Ashkin and W.J. Tomlinson, "Four-wave mixing in an artificial Kerr medium," *Opt. Lett.* **6**, 284-286 (1981).
3. A. Ashkin, J.M. Dziedzic and P.W. Smith, "Continuous-wave self-focusing and self-trapping of light in artificial Kerr media," *Opt. Lett.* **7**, 276-278 (1982).
4. V.E. Yashin, S.A. Chizhov, R.L. Sabirov, T.V. Starchikova, N.V. Vysotina, N.N. Rozanov, V.E. Semenov, V.A. Smirnov and S.V. Fedorov, "Formation of Soliton-like Light Beams in an Aqueous Suspension of Polystyrene Particles," *Opt Spectrosc+* **98**, 466-469 (2005).
5. P.J. Reece, E.M. Wright and K. Dholakia, "Experimental Observation of Modulation Instability and Optical Spatial Soliton Arrays in Soft Condensed Matter," *Phys. Rev. Lett.* **98**, 203902:1-4 (2007).
6. J.P. Gordon, "Radiation Forces and Momenta in Dielectric Media," *Phys. Rev. A* **8**, 14-21 (1973).
7. A. Ashkin, J.M. Dziedzic, J.E. Bjorkholm and S. Chu, "Observation of single-beam gradient force optical trap for dielectric particles," *Opt. Lett.* **11**, 288-290 (1986).
8. S. Stenholm, "The semiclassical theory of laser cooling," *Rev. Mod. Phys.* **58**, 699-739 (1986).
9. C. Conti, G. Ruocco and S. Trillo, "Optical Spatial Solitons in Soft Matter," *Phys. Rev. Lett.* **95**, 183902:1-4 (2005).
10. C. Conti, N. Ghofraniha, G. Ruocco and S. Trillo, "Laser Beam Filamentation in Fractal Aggregates," *Phys. Rev. Lett.* **97**, 123903:1-4 (2006).
11. R. El-Ganainy, K. G. Makris, D. N. Christodoulides, C. Rotschild, and M. Segev, "Cusp solitons in exponentially nonlinear nanosuspensions", paper QMB4, CLEO/QELS 2007, May 6-11, Baltimore, Maryland.
12. R. Gordon, J.T. Blakely and D. Sinton, "Particle-optical self-trapping," *Phys. Rev. A* **75** 055801:1-4 (2007).
13. D. Rogovin and S.O. Sari, "Phase conjugation in liquid suspensions of microspheres in the diffusive limit," *Phys. Rev. A* **31**, 2375-2389 (1985).
14. B.J. Berne and R. Pecora, *Dynamic Light Scattering: With Applications to Chemistry, Biology and Physics* (Dover Publication, Inc. New York 2000)
15. J.D. Jackson, *Classical Electrodynamics*, (John Wiley and Sons, New York 1999).
16. J.M.C. Garnett, "Colors in Metal Glasses and in Metallic Films," *Philos. Trans. R. Soc. London* **203**, 385-420 (1904).
17. J.M.C. Garnett, "Colors in Metal Glasses, in Metallic Films and in Metallic solutions," *Philos. Trans. R. Soc. London* **205**, 237- 288 (1906).
18. H.C. van de Hulst, *Light Scattering by Small Particles*, (Dover Publication, Inc. New York 1981).

19. N.G. Vakhitov and A.A. Kolokolov, "Stationary solutions of the wave equation in a medium with nonlinearity saturation," *Izv. Vyssh. Uchebn. Zaved Radiofiz.* **16** 1020 (1973) [*Radiophys. Quantum Electron.* **16**, 783-789 (1973)].
 20. L. Berge, "Wave collapse in physics: principles and applications to light and plasma waves," *Phys. Rep.* **303**, 259-370 (1998).
 21. M. Segev, G.C. Valley, B. Chosignani, P.D. Portp and A. Yariv, "steady state spatial screening solitons in photorefractive material with external applied field," *Phys. Rev. Lett.* **73**, 3211-3214 (1994).
 22. D.N. Christodoulides and M.I. Carvalho, "Bright, dark and gray spatial soliton states in photorefractive media," *J. Opt. Soc. Am B* **12**, 1628-1633 (1995).
 23. P.K. Kaw, K. Nishikawa, Y. Yoshida and A. Hasagawa, "Two-Dimentional and Three-Dimentional Envelope Solitons," *Phys. Rev. Lett.* **35** 88-91 (1975).
 24. J.Z. Wilcox and T.J. Wilcox, "Stability of Localized Plasma in Two and Three Dimentions," *Phys. Rev. Lett.* **34**, 1160-1163 (1975)
-

1. Introduction

Molecular kinetics plays a ubiquitous role in many and diverse areas of physics, chemistry, and life sciences [1]. Physical kinetics in particular is central in chemical reactions since it most directly determines the reactant concentrations. By their very nature, these are mesoscopic processes-all governed by statistical physics. Thus far, methods to regulate kinetic phenomena have relied on using traditional thermodynamic variables such as pressure, temperature, concentrations etc [1]. It will be certainly of importance to devise methods to optically control kinetic processes at a mesoscopic level. One possible avenue is to alter the local concentrations of nano-particle suspensions using optical beams. Yet, it is by now well known that, this same process will in turn affect the optical environment, thus leading to a mutual interaction between the beam itself and the nano-particle system. Following the pioneering work of Ashkin et al [2,3], the possibility of beam self-focusing and of four-wave mixing in artificial Kerr-like media involving nanosuspensions was considered in a number of experimental studies [2-5]. In such systems the optical nonlinearity is the direct outcome of the electromagnetic gradient force and can be relatively high depending on the size of the nano-particles involved [6-8]. From a practical perspective, such artificial nonlinear materials are quite attractive since nonlinear effects can be observed at very low power levels [2,3]. Interest in this area was recently rekindled in a number of new studies on both the theoretical [9,10] and the experimental [4,5] front. Nonetheless, it is important to emphasize, that so far, in most works the nonlinearity of nano-particle suspensions was a priori assumed to be of the Kerr type. Yet, as demonstrated in two theoretical studies [11,12], this rather simplistic assumption is only valid when the optical beam intensity is well below a threshold intensity set by the thermal energy. This in turn has important implications on nonlinear beam dynamics in such nano-suspension systems. In fact as demonstrated in [11,12], the nonlinearity of nanosuspensions varies exponentially with intensity. This exponential character of nonlinearity was also recognized in earlier studies using either thermodynamics arguments [2] or by invoking Chandrasekhar equation [13].

In this work, starting from first principles, we analyze the nonlinear response as well as the nonlinear Rayleigh losses associated with nano-particle suspensions. This is done by directly solving the underlying Nernst-Planck and Smoluchowski equations under equilibrium conditions. We show that in such systems both the optical nonlinearity and Rayleigh losses vary exponentially with optical intensity. Depending on the sign of the particle polarizability, these exponential nonlinearities can be saturable or monotonically increasing with intensity (unsaturable). The soliton solutions corresponding to these two cases are obtained and analyzed in detail. The stability properties of both 1D and 2D self-trapped states are investigated. Our analysis indicates that low power, relatively narrow soliton beams, can propagate undistorted over several diffraction lengths in spite of the presence of nonlinear Rayleigh scattering effects. In the case of negative polarizability particles, a self-induced transparency effect is predicted. The propagation characteristics of these self-localized beams are also investigated in nanosuspension mixtures with competing polarizabilities that can exhibit a novel nonlinear response.

2. Theoretical analysis

In this section we analyze the interaction between the electromagnetic field of a laser beam and the nanoparticles involved in a colloidal suspension. To do so we invoke the particle current continuity equation [14],

$$\frac{\partial \rho}{\partial t} + \nabla \cdot \vec{J} = 0, \quad (1)$$

where ρ represents the particle concentration and \vec{J} is the particle current density. In these systems, the mechanisms contributing to the particle current density are described by the Nernst-Planck equation [14]:

$$\vec{J} = \rho \vec{v} - D \nabla \rho, \quad (2)$$

where D is the diffusion coefficient and \vec{v} is the particle convective velocity which is related to the external force \vec{F} acting on the nanoparticles through the relation $\vec{v} = \mu \vec{F}$ where μ represents the particle's mobility. The first term on the right hand side of Eq. (2) gives the drift current due to the external force while the second one describes the diffusion current due to Brownian motion. In Eqs (1)-(2) we assume a highly diluted mixture and we neglect any particle-particle interactions. Combining Eqs. (1) and (2) one obtains the Smoluchowski equation, i.e.,

$$\frac{\partial \rho}{\partial t} + \nabla \cdot (\rho \vec{v} - D \nabla \rho) = 0. \quad (3)$$

In order to solve Eqs. (1-3) we assume steady state conditions, i.e. $\partial / \partial t = 0$. In addition, under equilibrium the current density is zero, $\vec{J} = 0$, i.e. drift is balanced by diffusion. In the case where the particle size is small compared to the wavelength (Rayleigh regime), the average optical gradient force on this nanoparticle can be obtained within the dipole approximation [6-8],

$$\vec{F} = \frac{\alpha}{4} \nabla I. \quad (4)$$

In Eq. (4), α represents the particle polarizability and the quantity $I = \vec{E} \cdot \vec{E}^*$ is associated with the light intensity through the peak spatial field amplitude \vec{E} . In the dipole approximation, the polarizability α of a spherical particle having a refractive index n_p is given by [15]:

$$\alpha = 3V_p \varepsilon_0 n_b^2 \left(\frac{m^2 - 1}{m^2 + 2} \right), \quad (5)$$

where $V_p = 4\pi a^3 / 3$ is the volume of the particle, ε_0 is the free space permittivity, n_b is the refractive index of the background medium and the dimensionless parameter $m = n_p / n_b$ represents the ratio of the particle's refractive index n_p to n_b . It is important to note that α can be positive or negative depending on whether the refractive index of the particle is higher ($m > 1$) or lower ($m < 1$) than that of the background.

In the absence of any illumination ($I=0$), $\vec{F} = \vec{v} = 0$, the particle density obeys Laplace's equation $\nabla^2 \rho = 0$ under steady state conditions. Moreover, at the container boundaries, the normal component of the diffusion current $\nabla \rho$ is zero. In this case, this Newman boundary value problem dictates that the particle density is everywhere constant. This uniform

distribution is also the one that leads to maximum entropy (in the absence of external constraints).

If on the other hand, light forces are present, substitution of Eq. (4) into Eq. (2) (under the condition $\vec{J} = 0$) leads to $(\alpha\mu/4)\rho\nabla I - D\nabla\rho = 0$. This last partial differential equation can be directly integrated and gives $\rho = \rho_0 \exp(\frac{\alpha\mu}{4D}I)$. From Einstein's relation $\mu/D = 1/k_B T$ we finally obtain:

$$\rho = \rho_0 \exp\left(\frac{\alpha}{4k_B T}I\right) \quad , \quad (6)$$

where $k_B T$ is the thermal energy and ρ_0 stands for the unperturbed uniform particle density (in the absence of light-when the container is large). Given the fact that $\frac{\alpha}{4}I$ is associated with the optical potential energy, this last result is another manifestation of the Boltzmann distribution in statistical physics [1]. Similarly the volume filling factor in nano-suspension systems follows a similar rule, that is $f(I) = f(0)\exp(\alpha I / 4k_B T)$. Moreover it is important to emphasize that this exponential law is only applicable in the case of relatively low concentrations (or filling factors) since the diffusion equation itself ignores particle-particle interactions. As we will see, in most typical cases Rayleigh scattering losses naturally provide an upper bound on particle concentration.

From Eqs. (5) and (6) we notice that the particle concentration will increase in the regions where the intensity is high, whenever the refractive index of the particles n_p is higher than that of the background n_b ($\alpha > 0$). The converse is true in the other regime ($\alpha < 0$), i.e. the particles will escape from the high intensity regions when their refractive index is lower than that of the surrounding medium. As a result the refractive index is locally perturbed due to this intensity dependent change in the particle concentration. To calculate this local index change we use the Maxwell-Garnett formula given by [16,17]:

$$n_{eff}^2 = n_b^2 \frac{n_p^2 + 2n_b^2 + 2f(n_p^2 - n_b^2)}{n_p^2 + 2n_b^2 - f(n_p^2 - n_b^2)} \quad . \quad (7)$$

In Eq.(7) n_{eff} is the effective refractive index of the medium and f is the volume filling factor given by the ratio of the volume of the particles to the total volume. If we expand the right hand side of Eq. (7) and by assuming a relatively small index contrast (i.e. $|m - 1|$ being small) we get:

$$n_{eff}^2 = n_b^2 \left(1 + 2f \frac{n_p - n_b}{n_b} \right) \quad . \quad (8)$$

In this same limit, Eq.(8) reduces to $n_{eff} = (1 - f)n_b + fn_p$. This result could have been intuitively anticipated based on fractional composition arguments. The change in the refractive index is then given by $\Delta n = n_{eff} - n_b = (n_p - n_b)f$ where the particle volume filling factor is defined as: $f = (\Delta N_p / \Delta V)V_p = \rho V_p$. This together with Eq. (6) provides the optical nonlinearity of such nanoparticle suspensions [11,12]:

$$\Delta n_{NL} = n_{eff}(I) - n_{eff}(I=0) = (n_p - n_b) V_p \rho_0 \left(e^{\frac{\alpha}{4k_b T} I} - 1 \right). \quad (9)$$

In addition to these nonlinear index changes, it is important to incorporate scattering losses in the dynamical evolution equations. If the particle size is smaller than the free-space wavelength λ_0 , the scattering cross section can be determined in the Rayleigh regime [18], that is:

$$\sigma = \frac{128 \pi^5 a^2 n_b^4}{3} \left(\frac{a}{\lambda_0} \right)^4 \left(\frac{m^2 - 1}{m^2 + 2} \right)^2, \quad (10)$$

where again a is the particle radius.

We now develop the beam evolution equation in nano-particle suspensions. Starting from the Helmholtz equation $\nabla^2 E + k_0^2 n_{eff}^2 E = 0$, and by assuming a slowly varying field envelope $\varphi(x, y, z)$, that is, $E(x, y, z) = \varphi(x, y, z) \exp(ik_0 n_b z)$, we find that:

$$i \frac{\partial \varphi}{\partial z} + \frac{1}{2k_0 n_b} \nabla_{\perp}^2 \varphi + k_0 (n_p - n_b) f \varphi + i \gamma \varphi = 0, \quad (11)$$

where γ in the last term represents the loss coefficient and $k_0 = 2\pi / \lambda_0$. If we now keep only the loss term in the last equation, we find that $|\varphi|^2 = |\varphi_0|^2 \exp(-2\gamma z)$. Given that $|\varphi|^2 = |\varphi_0|^2 \exp(-\alpha_l z)$ where the loss coefficient is given by $\alpha_l = \sigma \rho$ we finally obtain $2\gamma = \sigma \rho = \sigma \rho_0 \exp(\alpha I / 4k_b T)$. This final expression for the loss coefficient is important since it demonstrates that the scattering losses are actually nonlinear, i.e. they depend on the beam intensity. As will be shown later, these nonlinear Rayleigh losses will play a crucial role in the beam propagation dynamics. From these latter results, Eq. (11) takes the form:

$$i \frac{\partial \varphi}{\partial z} + \frac{1}{2k_0 n_b} \nabla_{\perp}^2 \varphi + k_0 (n_p - n_b) V_p \rho_0 e^{\frac{\alpha}{4k_b T} |\varphi|^2} \varphi + \frac{i}{2} \sigma \rho_0 e^{\frac{\alpha}{4k_b T} |\varphi|^2} \varphi = 0. \quad (12)$$

Note that equation (12) is general and is applicable in both cases irrespective of whether the polarizability α is positive or negative. If we first consider the case of positive polarizability and by introducing the following normalizations, $\xi = z / 2k_0 n_b w^2$, $X = x / w$, $Y = y / w$, $w^{-2} = 2k_0^2 n_b |n_p - n_b| V_p \rho_0$, $\varphi = (4k_b T / |\alpha|)^{1/2} U$, Eq.(12) takes the form:

$$i \frac{\partial U}{\partial \xi} + U_{XX} + U_{YY} + e^{|U|^2} U + i \delta e^{|U|^2} U = 0, \quad (\text{for } n_p > n_b) \quad (13)$$

In Eq.(13) U is the normalized field amplitude, w is a characteristic beam width, and the normalized loss δ is given by $\delta = \sigma / (2k_0 |n_p - n_b| V_p)$. In the same manner, if the polarizability is negative, we obtain

$$i \frac{\partial u}{\partial \xi} + u_{XX} + u_{YY} - e^{-|u|^2} u + i \delta e^{-|u|^2} u = 0, \quad (\text{for } n_p < n_b) \quad (14)$$

where here we used the symbol u instead of U . If now introduce the transformation $u = Ue^{-i\xi}$ in equation (14) we obtain:

$$i \frac{\partial U}{\partial \xi} + U_{XX} + U_{YY} + \left(1 - e^{-|U|^2}\right)U + i\delta e^{-|U|^2}U = 0 \quad , \quad (\text{for } n_p < n_b). \quad (15)$$

Equations (13) and (15) are normalized evolution equations describing wave propagation in these two different cases.

Note that in both situations the nonlinearity is of the self-focusing type. In the first case, described by Eq. (13), the nonlinearity is monotonically exponential. On the other hand, in the second regime (Eq.(15)), the nonlinearity is exponentially saturable. Even though at first sight it might be unclear how both systems lead to a self focusing nonlinearity, this can be clarified using the following physical arguments. In the case where the particles have a higher refractive index than the background, the polarizability α of each particle is positive and thus the particles are attracted toward the high intensity region, i.e. to the center of the beam, thus elevating the effective refractive index of the system (Fig. 1(a)). This will of course increase the nonlinear scattering losses as well. On the other hand, particles having a lower refractive index than that of the background and hence a negative polarizability will be repelled away from the center of the beam, again raising the refractive index at the center (Fig. 1(b)). In this latter case however, the nonlinear losses decrease at the beam center (due to the reduction in the particle concentration), thus increasing the transparency of the system. As it will be shown, this difference in the character of the exponential optical nonlinearity will have a profound effect on the beam dynamics of spatial solitons.

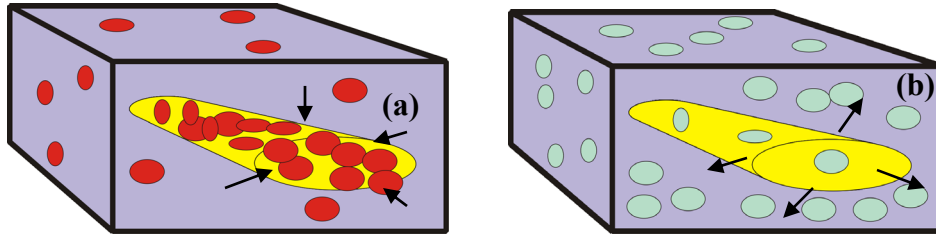


Fig. 1 A high intensity beam (a) attracting nanoparticles with positive polarizabilities and (b) repelling nanoparticles with negative polarizabilities.

3. Soliton dynamics and stability properties

In this section we investigate the dynamics and stability properties of the soliton solutions possible in exponentially nonlinear nano-suspensions. To do so, we solve Eqs. (13) and (15) in both one and two dimensional configurations in the absence of any nonlinear Rayleigh losses ($\delta = 0$).

3.1 1D soliton solutions

We first consider the 1D case. Here we seek 1D stationary solutions of the form $U(X, \xi) = g(X)\exp(i\kappa\xi)$ where κ represents the soliton eigenvalue. Substituting this latter expression into Eqs. (13) and (15) gives:

$$g_{XX} - \kappa g + e^{g^2} g = 0 \quad , \quad (16-a)$$

$$g_{XX} - \kappa g + \left(1 - e^{-g^2}\right)g = 0 \quad (16-b)$$

Equations (16) can be readily integrated once, thus leading to:

$$g_X^2 - \kappa g^2 + e^{g^2} = C_1 \quad (17-a)$$

$$g_X^2 + (1 - \kappa)g^2 + e^{-g^2} = C_2 \quad (17-b)$$

Since asymptotically, these solutions satisfy $g|_{X \rightarrow \infty} = 0$ and $g_X|_{X \rightarrow \infty} = 0$, we set $C_1 = C_2 = 1$. By rearranging Eqs.(17) we directly obtain:

$$\int_{g_0}^g \frac{dg'}{\sqrt{1 + \kappa g'^2 - \exp(g'^2)}} = \pm \int_0^X dX' \quad (18-a)$$

$$\int_{g_0}^g \frac{dg'}{\sqrt{1 + (\kappa - 1)g'^2 - \exp(-g'^2)}} = \pm \int_0^X dX' \quad (18-b)$$

As Eqs. (18) imply, these soliton solutions are symmetric with respect to the origin $X = 0$. Using the boundary conditions at the beam center, namely that $g(0) = g_0$ and $g_X(0) = 0$ we can now numerically integrate Eqs. (18).

We will first discuss the 1D soliton solutions associated with exponential nonlinearities, i.e., Eq. (18-a). Figure 2(a) shows the existence curve of these solutions, e.g. their normalized intensity FWHM as a function of their peak intensities. The inset in Fig. 2(a) shows the intensity profile of such a solution at $\kappa = 3$. As one can see, the beam width monotonically decreases as the soliton peak intensity increases. The stability properties of this class of solutions can be systematically examined using the power-eigenvalue ($P - \kappa$) diagram where $P = \int |U|^2 dX$. Following Vakhitov and Kolokolov [19], this solution is stable whenever the slope of the curve is positive (for $\kappa < 2.49$) and is unstable for higher eigenvalues where the slope is negative as shown in Fig. 2(b).

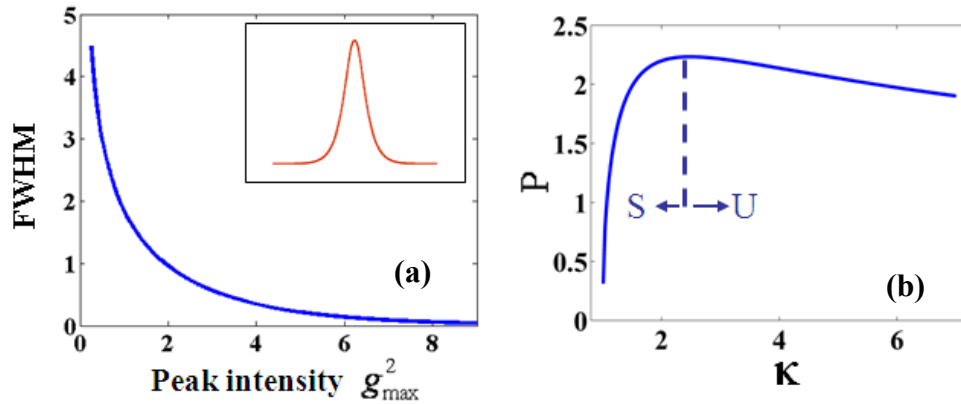


Fig. 2 Normalized soliton FWHM width as a function of their normalized peak intensities in exponential nonlinear nanosuspensions. The inset represents the intensity profile of such a solution. (b) The corresponding $P - \kappa$ diagram with S being the stable and U the unstable branch.

The existence of two different regions of stability is by itself an interesting result given that we are dealing with a 1D system [20]. In reality, above this threshold ($\kappa = 2.49$) these 1D solutions tend to catastrophically collapse into a singularity. This behavior can be qualitatively

explained based on the Taylor series expansion $e^{|U|^2} = 1 + |U|^2 + (1/2)|U|^4 + \dots$. As a result, at lower intensities the nonlinearity is of the Kerr-type and the corresponding solutions are stable. However, at higher intensities, the degree of nonlinearity is above the supercritical value (i.e. $|U|^4$) necessary for 1D systems to exhibit collapse [20]. Of course in reality nonlinear Rayleigh scattering and/or saturation effects in the particle concentration will prevent such a collapse from occurring. The dynamics of these solutions are then studied by directly solving Eq. (13) and by including nonlinear Rayleigh scattering losses. To illustrate our results we consider the propagation of a soliton beam in nano-suspensions when the wavelength is $0.532 \mu m$. The nano-suspensions involve polystyrene nano-particles (refractive index $n_p = 1.56$) of radius $50 nm$ suspended in water ($n_b = 1.33$) at a concentration of $7 \times 10^{11} cm^{-3}$ (or $f = 3.5 \times 10^{-4}$). Under linear conditions, a 10 micron beam (FWHM in width) expands considerably because of diffraction (3 times) and loses 13% of its power because of scattering losses. Conversely, in the nonlinear regime, this same beam can propagate up to 4 diffraction lengths ($2 mm$) without any appreciable distortion-limited only by the nonlinear losses (20%), as clearly shown in Fig. 3.

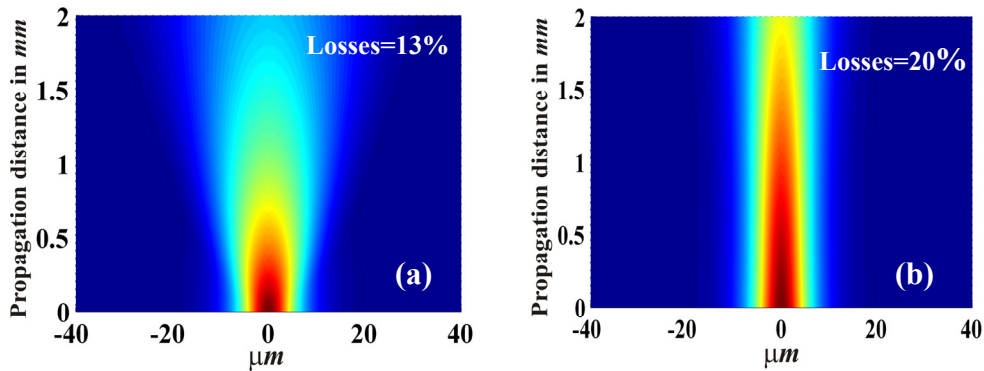


Fig. 3(a) Linear propagation of an optical beam in water-polystyrene nanosuspension. (b) Nonlinear soliton effects in this same system.

On the other hand, the situation for the saturable nonlinearity (described by Eqs. (15) and (18-b)) is quite different. Figure 4(a) shows the soliton existence curve for this latter system.

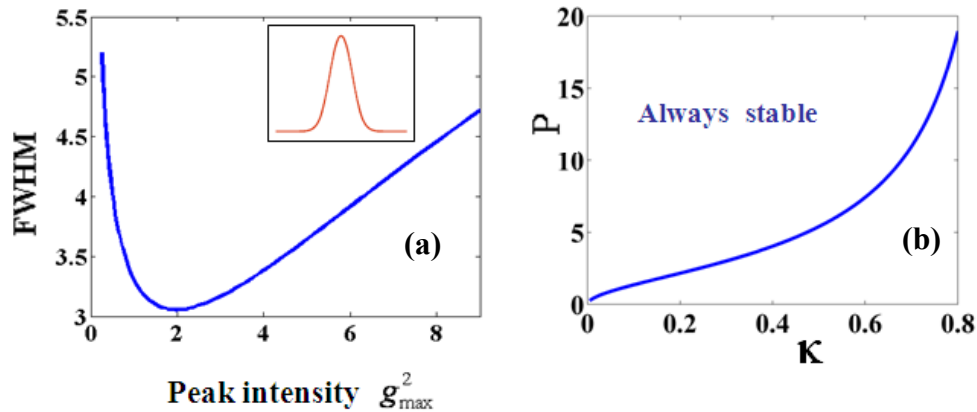


Fig. 4(a) Normalized soliton intensity FWHM width as a function of their peak intensity in exponentially saturable nanosuspensions. The inset depicts such a solution (b) Corresponding $P - \kappa$ diagram indicating stability.

These results indicate that the intensity FWHM width of these solutions tend to initially contract with peak intensity and eventually expand –a characteristic behavior of solitons in saturable systems [21,22]. The inset in Fig. 4(a) shows the intensity profile of such a solution at $\kappa = 0.95$. The power-eigenvalue $P - \kappa$ diagram in this regime is shown in Fig. 4(b). This graph indicates that in the saturable case (of negative polarizabilities) the 1D soliton solutions are always stable since $dP/d\kappa > 0$.

Figure 5 depicts the propagation of a 10 micron beam (FWHM in width) in a suspension involving 50 nm air nano-bubbles ($n_p = 1$) floating in water ($n_b = 1.33$). Again the wavelength is taken to be $0.532 \mu\text{m}$. The nano-bubble concentration is assumed to be $2 \times 10^{12} \text{ cm}^{-3}$ or $f = 10^{-3}$. Under linear or low power conditions, the beam diffracts considerably (more than 10 times) and loses almost all its energy (97%) as clearly indicated in Fig. 5(a).

This considerable loss is a direct outcome of Rayleigh scattering at these concentration numbers. At power levels sufficient to sustain a soliton however, the beam expels the nanospheres from the center, thus giving rise to *self-induced transparency* and self-trapping effects. In other words, at high powers the beam can effectively reduce the “haze” while at the same time can establish its own waveguide structure. In this case the overall losses drop from 97% to 20%. A direct simulation of this beam (based on Eq. (15)) shows that the soliton (10 micron FWHM) can propagate up to 12 diffraction lengths (Fig. 5(b)), i.e. approximately 4 times more than in the first case. This behavior is understood by recalling that the nonlinear losses are exponentially growing in the first case whereas are exponentially decaying in the second one.

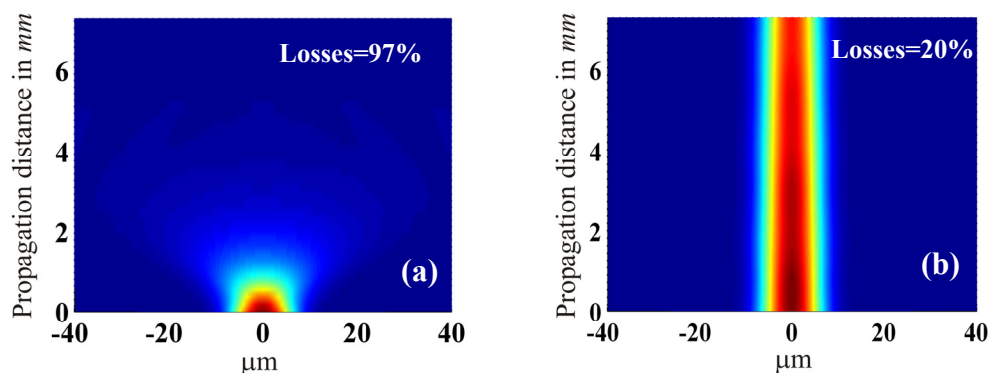


Fig. 5 Linear propagation of a 10 μm beam in water-air nanobubble suspensions where 97% of losses are expected. (b) Nonlinear soliton self-trapping and self-induced transparency effects.

3.2 2D soliton solutions

Two-dimensional soliton solutions in these systems are obtained by directly solving the 2D version of Eqs.(13) and(15). To do so we seek stationary solutions in cylindrical coordinates having the form $u(r, \xi) = g(r)\exp(i\kappa\xi)$ and we keep in mind the boundary conditions $g = 0$ at $r \rightarrow \infty$ and $dg/dr = 0$ at $r = 0$.

We begin by considering first nanoparticles with positive polarizabilities. In this regime, the normalized ($P - \kappa$) diagram associated with these solutions is shown in Fig. 6(a). The monotonically decreasing behavior of this latter curve clearly indicates that the 2D soliton solutions in exponentially nonlinear nanosuspensions are always unstable and tend to

catastrophically collapse. Again as in the 1D case, collapse will be prevented because of nonlinear Rayleigh scattering and/or saturation effects in the particle concentration. In addition, the intensity profiles of this class of waves exhibit a cusp-like shape as a result of the exponential nonlinearity, as shown in Fig. 6(b). As an example we study the propagation of a 10 micron width (FWHM) 2D beam in water containing polystyrene nanospheres. All the physical parameters are the same as those used in the corresponding 1D system except for the volume filling factor which taken here to be $f = 10^{-4}$. At low power levels the beam expands because of diffraction (2 times) and loses 2% of its power as a result of Rayleigh scattering, as shown in Fig. 6(c). On the other hand, at 5W (at soliton power), this same beam can propagate up to 1mm (3.5 diffraction lengths) without any appreciable expansion and in spite of the nonlinear Rayleigh losses (5%) as accounted in Eq.(13), as demonstrated in Fig. 6(d). We note that in our simulations this beam would have otherwise undergone a collapse had not been for Rayleigh scattering. This collapse behavior is illustrated in Fig. 6(e) in the absence of nonlinear losses and by neglecting saturation effects in the particle density.

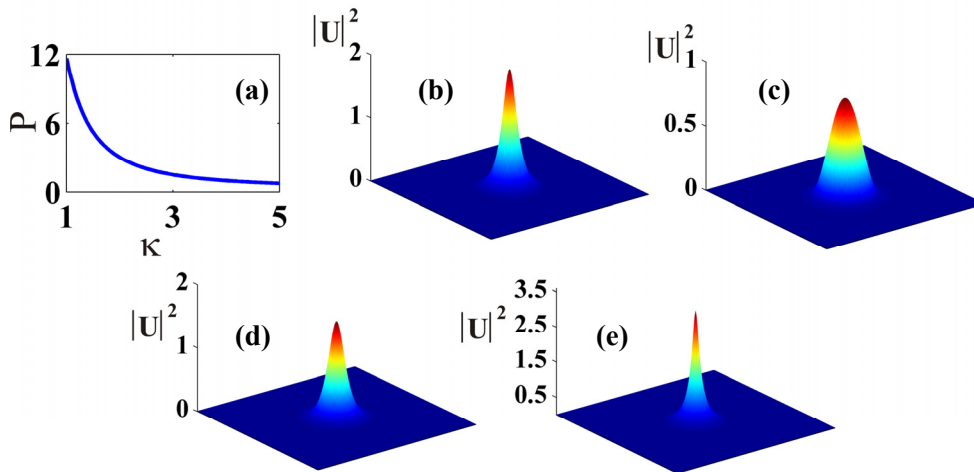


Fig. 6(a) $P - \kappa$ stability diagram of 2D solitons in nanosuspensions with positive polarizabilities. (b) Soliton intensity profile at $\kappa = 1.7$. (c) Beam diffraction at low power levels shown in scale. (d) Propagation dynamics of a 2D 10 μm soliton beam after 1 mm in the presence of Rayleigh losses. (e) Catastrophic collapse in the absence of nonlinear losses.

We now consider 2D soliton solutions in nanosuspensions with negative polarizabilities exhibiting saturable exponential nonlinearities similar to those encountered in plasma science [23,24]. This is done by considering Eq. (15) in the absence of losses. The $(P - \kappa)$ stability diagram associated with these solutions is shown in Fig. 7(a) and indicates that these self-trapped states are always stable since $dP/d\kappa > 0$.

To illustrate our results we consider air nano-bubble suspensions in water. Again all the physical parameters used here are the same as those used in the corresponding 1D example and $f = 10^{-3}$. Fig. 7(b) shows the intensity profile of a 10 μm beam (FWHM) that is possible in this system at a power level of 2.8 Watts. At very low intensities, after 3.5 mm of propagation, the beam linearly diffracts (7 times) and loses 80% of its power because of substantial Rayleigh scattering, Fig. 7(c). On the other hand, when the beam input power is 6 W, the beam self-traps and at the same time increases the transparency of the system by optically expelling the nanoparticles from its center. In this latter case, the beam expands only by 10% and loses a small fraction of energy (20%) after 3.5 mm of propagation as shown in

Fig. 7(d). As in the 1D case, this self-induced transparency effect is again a result of the specific nature of the optical gradient force.

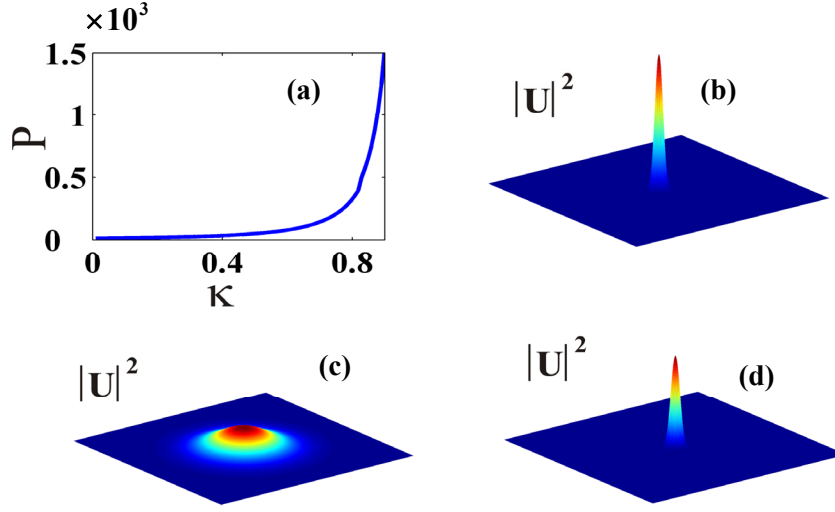


Fig. 7(a) $P - \kappa$ stability diagram of 2D solitons in nanosuspensions with negative polarizabilities. (b) Soliton intensity profile at $\kappa = 0.5$. (c) Expansion and loss effects during linear propagation of a 2D 10 μm beam after 3.5 mm (d) Self-trapping and self-induced transparency effects at 6 W of beam power in this same system.

4. Engineering nonlinearities in nano-suspension systems

So far we have considered nano-suspensions involving only one type or species of nano-particles. In this section we study the effect of mixing two or more types of nano-particles in the same suspension. In this case the Nernst-Planck equation takes the form:

$$\vec{J} = \sum_j \vec{J}_j = \sum_j (\rho_j \vec{v}_j - D_j \nabla \rho_j) \quad , \quad (19)$$

where the subscript j runs over all different kinds of nano-particles. In the case of diluted suspensions particle-particle interactions can be neglected. As a result each current component \vec{J}_j vanishes independently and the statistical distribution for each type of nano-particles is represented by a Boltzmann distribution, i.e.

$$\rho_j = \rho_{j0} \exp\left(\frac{\alpha_j}{4k_B T} I\right) \quad . \quad (20)$$

Following an analysis similar to that of section 2, we find that the beam evolution equation in such a system is given by:

$$i \frac{\partial U}{\partial \xi} + U_{xx} + U_{yy} + \sum_{j=1,2,3,\dots} \left[\frac{(n_{pj}^+ - n_b)V_j^+ \rho_{jo}^+}{(n_{p1}^+ - n_b)V_1^+ \rho_{io}^+} e^{\frac{\alpha_j^+}{\alpha_1^+} |U|^2} U + \frac{(n_b - n_{pj}^-)V_j^- \rho_{jo}^-}{(n_{p1}^- - n_b)V_1^- \rho_{io}^-} \left(1 - e^{-\frac{|\alpha_j^-|}{\alpha_1^-} |U|^2}\right) U \right] + \sum_{j=1,2,3,\dots} i \left(\frac{\delta_j^+}{\delta_1^+} e^{\frac{\alpha_j^+}{\alpha_1^+} |U|^2} + \frac{\delta_j^-}{\delta_1^-} e^{-\frac{|\alpha_j^-|}{\alpha_1^-} |U|^2} \right) U = 0 \quad . \quad (21)$$

In Eq. (21), we have incorporated nonlinear contributions from either type of particles, i.e. from those with positive or negative polarizabilities (the +/- superscript denotes particles with positive/negative polarizabilities). The last term in Eq.(21) represents Rayleigh losses due to these two different kinds of nano-particles. For each family, the equation implicitly assumes different values for their respective polarizabilities and densities. Note that in Eq.(21) the coefficient of each term is a function of the nano-particle properties (refractive index, radius) and their concentrations. Thus by controlling these parameters one could design an otherwise nonexistent nonlinear response. For example if we consider a mixture of only two different types of particles having equal but opposite polarizabilities and we choose the particle concentrations so as the nonlinear coefficients in both terms of Eq.(21) are equal to unity, then the nonlinear evolution equation (neglecting the loss terms) can take the form:

$$i \frac{\partial U}{\partial \xi} + U_{xx} + U_{yy} + 2 \sinh(|U|^2) U = 0 \quad . \quad (22)$$

This suggests that systems with artificial nonlinearities (such as that of Eq.(22) with sine-hyperbolic nonlinearity) can be for example synthesized at will through appropriate inclusion of nanoparticles.

5. Conclusion

In conclusion we have demonstrated that the interaction of an optical beam with nanoparticle colloidal suspensions leads to exponential self-focusing nonlinear effects as well as exponential Rayleigh scattering losses. This system was investigated in two different regimes depending on whether the nanoparticle polarizability is positive or negative and was shown that altogether different behavior is expected in each case. Soliton dynamics and their stability properties were analyzed in these two cases for both 1D and 2D configurations and it was demonstrated that by taking into account nonlinear Rayleigh losses soliton collapse can be prevented. Our analysis revealed that apart from self-trapping, another very interesting phenomenon can be expected-that of self-induced transparency, as long as the nanoparticle polarizability is negative. In addition we considered the possibility of synthesizing new nonlinearities by using mixtures of different types of nanoparticles. We would like to note that several other issues merit further investigation. These include for example system dynamics under non-equilibrium conditions, particle-particle interactions in high density suspensions, and particle distribution in the presence of non-conservative force fields. Finally effects arising from temperature gradients, viscosity etc may need attention. We intend to address these aspects in future work.